Integrated Control Strategy for Islanded Operation in Smart Grids: Virtual Inertia and Ancillary Services

Simone Negri
Student Member, IEEE
DEIB
Politecnico di Milano
Piazza Leonardo da Vinci, 32
Milan, 20133, Italy
simone.negri@polimi.it

Enrico Tironi
DEIB
Politecnico di Milano
Piazza Leonardo da Vinci, 32
Milan, 20133, Italy
enrico.tironi@polimi.it

Davide Sala Danna
Engineering Department
Acrotecna srl
Via Grado, 12
Meda (MB), 20821, Italy
davide.saladanna@acrotecna.it

***Abstract*— Distributed Generation has become a consolidated phenomenon in distribution grids in the last few years. Even though the matter is very articulated and complex, islanding operation of distribution grid is being considered as a possible measure to improve service continuity. In this paper a novel static converter control strategy to obtain frequency and voltage regulation in islanded distribution grid is proposed. Two situations are investigated: in the former one electronic converter and one synchronous generator are present, while in the latter only static generation is available. In the first case converter control will realize virtual inertia and efficient frequency regulation by mean of PID regulator; this approach allows to emulate high equivalent inertia, hence limiting the ROCOF and maximum frequency deviation, and, in the meantime, to obtain faster frequency regulation, which could not be possible with traditional regulators. In the second situation a Master-Slave approach will be adopted to maximize frequency and voltage stability. Even though the presented results are obtained in a grid with only two generators, the proposed approach can be extended to more general configurations with few generation units. Simulation results confirm that the proposed control allows islanded operation with high frequency and voltage stability under heavy load variations.**

***Keywords*— virtual inertia; smart grid; islanded grid operation; ancillary services;**

I. INTRODUCTION

Distributed Generation has been having a growing impact on distribution grids in the last few years. More and more active users are hence involved in grid dynamics, but, because of normative and technical issues, they are not involved in grid management. In order to improve service continuity, active users and generators should be involved in an integrated grid management strategy [1]-[3]; this approach, with particular attention to islanded operation, can be a key to evolve from traditional grids to smart grids. Moreover, active users are not highly involved in frequency regulation – in fact, only active power modulation during frequency transients is foreseen [4]-[6]. Among many available studies, two main approaches are recognizable: some of them [7]-[19] are aimed to control static converters in order to emulate synchronous generators behaviour, especially during grid transients and with particular attention to inertia emulation [20]- [27]; other studies [28]-[34] are aimed to realize efficient micro-grid control with high frequency and voltage stability, obtained mostly through a droop control or master-slave approach. The emulation of synchronous generators allows easy and effective integration of renewable energy sources with the main grid; furthermore, virtual synchronous generators can participate to frequency and voltage regulation as traditional ones. These considerations led to different synchronous generator emulation solutions, from the synchronverter [7]-[10] to more general virtual synchronous generators [11]-[19]; in the latter, different levels of synchronous generators modelling are used, ranging from the complete model to the bare mechanical/inertia emulation. In particular, a first formulation of the synchronverter is presented in [7], while [8]-[10] present updated and improved iterations addressing specific issues of the original formulation. A similar approach has also developed under the name of virtual synchronous generator [11]-[16]. In [11] an overview on synchronous generator emulation is presented, while some newer perspectives in VSG control, with particular reference to oscillation damping, is reported in [13], [14]. More recent high-voltage applications are presented in [15]-[17]. Note that, for some applications, storage devices may be necessary to perform synchronous generators emulation - examples can be found in [18], [19]. Some other papers [20]-[26], on the contrary, focus only on inertia emulation, neglecting the electrical part of the synchronous generators model: this approach produced results both for micro-grid [20]-[22] and power systems [23] applications. Wind turbines can also be considered as sources of virtual inertia, as reported in [24],[25], while a basically different approach, more similar to an induction machine than a synchronous generator, is proposed in [26]. Nevertheless, synchronous generator emulation does not completely take advantage of the high dynamic performances of static converters. Furthermore, when micro-grids are considered, a two-fold scope is pursued: on one side, high-performance frequency and voltage control is generally requested, while, on the other side, a general simplification in system control is desired. These considerations cast a growing interest on alternative approaches in micro-grids control and operation, mainly ascribable to droop [28]-[31] or master–slave [32],[33] control; an interesting comparison between synchronous generator emulation and droop control is reported in [34]. Secondary regulation and hierarchical control structures are also proposed in [28], [35]-[37].

In this paper a novel static converter control strategy to obtain frequency and voltage regulation in islanded distribution grid is proposed. A small medium-voltage islanded grid will be

considered as case study and two situations are investigated: in the former one synchronous generator and one static converter are connected to the grid, while in the latter only two static converters are present. In both cases, converters are supposed to be powered by active DC micro-grids [1],[3] and transition from grid connected to islanded operation and vice versa will not be considered.

In the first case, due to the presence of a prevalent synchronous generator, a single regulator will be designed to perform inertia emulation and effectively contribute to frequency regulation, overcoming the machine/governor emulation in VSGs and steady state errors of droop control; this approach allows to emulate high equivalent inertia, hence limiting the ROCOF and maximum frequency deviation, and, in the meantime, to obtain faster frequency regulation, which could not be possible with traditional regulators. In order to allow for secondary regulation, in particular in case storage devices are used, a second regulator is added to control steady-state active power injection. The proposed control introduces a significant difference from the general inertia/synchronous generation emulation in that an integral term is introduced to control how the frequency nominal value is restored, but still the converter contribution is limited to transients due to the presence of the secondary regulator; furthermore, even if a supervisory control layer may be necessary to obtain economic load sharing, the proposed solution allows to fully exploit the converter dynamic capability enhancing grid stability, reducing frequency deviation and assuring zero steady-state frequency error. In the second case, being the micro-grid fed by static converter only, there is no need to reduce the converter bandwidth introducing inertia or synchronous machine emulation as long as the converters are correctly controlled; hence a master-slave approach is adopted to maximize frequency and voltage stability. The master converter will be operated at fixed frequency, so that there is no need for frequency regulation and grid transients are reduced to voltage transients. In comparison to droop control, this approach allows to obtain greater voltage and frequency stability with zero steady-state error. Achieving economic power sharing may require a supervisory control layer, but other control approaches would require secondary regulation, so that there is no significant difference in control complexity.

This paper is organized as follow: Section II presents the problem statement and grid topologies, Section III illustrates control strategies for both situations, Section IV reports discussion on control stability, Section V presents the considered case studies and relative data, Section VI reports the main simulation results and final conclusions are presented in Section VII.

II. Problem Statement

A. Voltage and frequency regulation in micro-grids with prevalent synchronous generation

The first considered grid topology is shown in Fig.1,a and consists of a medium-voltage islanded feeder. Three loads are connected to the grid, which is fed by two active users, one inverter and one synchronous generator, supposed to be a regulating group. The main issue for grid operation is frequency regulation since, even though the speed governor of the synchronous generator can effectively restore nominal frequency after transients, the relatively reduced inertia of the system can lead to large frequency transients. Voltage regulation, on the contrary, is not critical.

B. Voltage and frequency regulation in micro-grids with little or no synchronous generation

The grid topology considered for this second case study is reported in Fig.1,b and is equivalent to study case A except from active users. Due to the substantial absence of rotating machines, frequency control is not critical, in that it is not related to mechanical constraints and grid can be operated at constant frequency; consequently, grid stability is reduced to voltage stability. Note that this situation can be easily generalized to grids in which minor synchronous generators are present or to grids comprising non-regulating synchronous generators.

III. Control Strategies

A. Voltage and frequency regulation in micro-grids with prevalent synchronous generation

In this first case, the synchronous generator is assumed to be equipped with a suitable speed governor and static exciter; the speed governor [38] can be modelled as

$$G_{Gov}(s) = \frac{P_n}{\omega_S} \cdot \frac{k_{g1}\left(1+sT_{g1}\right)}{s^2T_{g1}+s\left(1+k_{g2}T_{g1}\right)} \tag{1}$$

where k_{g1}, k_{g2}, T_{g1} are coefficients depending on the governor construction; the static excitation [38] can be modelled as

$$G_{Ex}(s) = \frac{k_e\left(1+sT_{e1}\right)}{s\left(1+sT_{e2}\right)} \tag{2}$$

where k_e, T_{e1}, T_{e2} are the excitation gain and time constants. The proposed strategy for inverter integration in frequency and voltage regulation consists of a current controlled inverter which, following grid voltage and frequency, injects active power to contrast frequency variations and reactive power to contrast voltage variations. A space-vector approach [39] is considered for compact and general three-phase system modelling. Current control is realized through a Smart Modulation algorithm, which allows to obtain direct current control and constant switching frequency [40],[41], and an inverse dynamic approach will be considered in order to compensate the output filter and transformer dynamics. This technique, largely applied in robot manipulators control, allows to transform a Multi-Input-Multi-Output coupled system into a set of linear decoupled systems by mean of a suitable feedback. Even though simpler control approaches (i.e. PI-based decoupled control) may produce good results [42], the inverse dynamic approach allows to compensate the natural oscillations of the filter and hence to ensure better dynamic performances. The converter topology considered for control synthesis is shown in Fig.2 and consists of a standard two level, low voltage inverter. However, the proposed control does not depend on converter topology except from the modulation

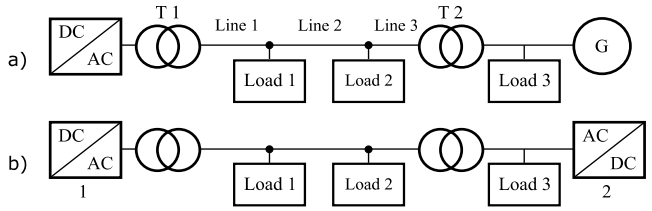

Figure 1 – a) first and b) second considered grid topologies

algorithm, which can be reformulated for different topologies. The LCL output filter is constituted by the filter inductance L_s, the filter capacitor C and the transformer inductance L_g. Transformer winding resistances, magnetization inductance and iron losses are neglected for simplicity; anyway, they proposed approach can be easily adapted to consider those parameters. Considering grid voltage space vector $\boldsymbol{v}_g$ as phase reference, reference currents can be obtained in *d-q* domain as

$$\boldsymbol{i}_{g\,ref} = \frac{2}{3}\left(\frac{P_{ref}}{\boldsymbol{v}_{gd}} + j\frac{Q_{ref}}{\boldsymbol{v}_{gd}}\right) \tag{3}$$

where $\boldsymbol{i}_{g\,ref}$ is the reference current space vector and P_{ref}, Q_{ref} are the reference active and reactive power. Note that, being the reference current $\boldsymbol{i}_{g\,ref}$ calculated from the measured grid voltage, active and reactive power injected from the converter are naturally decoupled. The reference current space vector $\boldsymbol{i}_{s\,ref}$ can be obtained by mean of an inverse dynamic approach. Defining the current tracking error as

$$\varepsilon_i = \boldsymbol{i}_{g\,ref} - \boldsymbol{i}_g \tag{4}$$

it is then possible to write the dynamic current error equation

$$\eta_i = \varepsilon_i + T_{i1}\cdot\dot{\varepsilon}_i + T_{i2}\cdot\ddot{\varepsilon}_i + \frac{1}{T_{i3}}\int \varepsilon_i\, dt \tag{5}$$

where T_{i1}, T_{i2}, and T_{i3} are coefficients to be chosen in order to obtain the desired damping and dynamic response. Derivatives of the tracking error are present with order up to the relative order of the system to obtain explicit dependence from the control variable $\boldsymbol{i}_s$. However, error derivatives do not have to be numerically computed: in fact, considering inductors and capacitors constitutive relations, it is not difficult to prove that

$$\dot{\varepsilon}_i = \dot{\boldsymbol{i}}_{g\,ref} + \frac{1}{L_g}\left(\boldsymbol{v}_g - \boldsymbol{v}_c\right) + j\omega\boldsymbol{i}_g \tag{6}$$

$$\ddot{\varepsilon}_i = \ddot{\boldsymbol{i}}_{g\,ref} + \frac{1}{L_g}\dot{\boldsymbol{v}}_g + \frac{1}{L_g C}\left(\boldsymbol{i}_g - \boldsymbol{i}_s\right) + j\frac{2\omega}{L_g}\boldsymbol{v}_c - j\frac{\omega}{L_g}\boldsymbol{v}_g + \omega^2\boldsymbol{i}_g \tag{7}$$

where $\boldsymbol{v}_c$ is the capacitor voltage space vector and ω is the system angular frequency.

In (6), (7) only the reference current and grid voltage derivatives are present: the former can be easily calculated since the current reference is calculated in the control, while the latter can practically be neglected with little or no impact on dynamic performance. Substituting (4), (6) and(7) in (5) and imposing $\eta_i=0$ and $\boldsymbol{i}_s = \boldsymbol{i}_{s\,ref}$, it is possible to obtain the current reference $\boldsymbol{i}_{s\,ref}$ as

$$\begin{aligned}\boldsymbol{i}_{s\,ref} = &\left[L_g C\ddot{\boldsymbol{i}}_{g\,ref} + C\dot{\boldsymbol{v}}_g + \boldsymbol{i}_g + j\omega C\boldsymbol{v}_g + \omega^2 L_g C\boldsymbol{i}_g\right] + \\ &+ g_{i1}\left[L_g C\dot{\boldsymbol{i}}_{g\,ref} + C\left(\boldsymbol{v}_g - \boldsymbol{v}_c\right) + j\omega L_g C\boldsymbol{i}_g\right] + \\ &+ g_{i2}L_g C\left(\boldsymbol{i}_{g\,ref} - \boldsymbol{i}_g\right) + g_{i3}L_g C\int\left(\boldsymbol{i}_{g\,ref} - \boldsymbol{i}_g\right)dt\end{aligned} \tag{8}$$

where gains are defined as $g_{i1}=T_{i1}/T_{i2}$, $g_{i2}=1/T_{i2}$, $g_{i3}=1/T_{i2}T_{i3}$. It is possible to determine gain values considering (5) in frequency domain and imposing $\eta_i=0$; it is not difficult to prove that optimal damping is obtained when $g_{i1}=3/T$, $g_{i2}=3/T^2$ and $g_{i3}=1/T^3$, where T is the desired system time constant to be set considering the desired dynamic performances. A suitable range for time constant tuning is $T \in [0.001,\ 0.004]$ *s,* in which the upper bound is set in order to reach steady-state condition within one period of the fundamental frequency, while the lower bound is set to avoid interference of switching dynamics in the control loop. Note that this approach reduces three independent gain choices to a single time constant choice, hence reducing the degrees of freedom of the problem; anyway, at least for this application, this leads to satisfactory performances. Overall, the control is equivalent to a PID regulator with a feed-forward/compensation term: in (8) the first term can be considered a feed-forward/compensation term, while the second, third and fourth terms are, respectively, derivative, proportional and integral terms, even though the current tracking error derivative is mostly obtained analytically. Anyway, this approach allows to directly obtain optimal gains and feed-forward/compensation terms with no need for complete closed-loop analysis. The impact of the proposed method on the stability of the system will be discussed in the Section IV, B. Defined the lower level of control, it is necessary to build reference active and reactive power to obtain voltage and frequency regulation. For these purposes, the grid will be considered prevalently inductive; anyway, the proposed control is barely affected by grid impedance as long as it is not prevalently resistive (i.e. as long as it is possible to control grid frequency by mean of active power). Voltage regulation can be generally realized locally or centralized: if centralized, a reference reactive power will be provided by the Distribution System Operator (DSO), while, if locally realized, a reference voltage should be provided. If a reactive power reference is provided, it can be directly used in (3) to obtain reference currents; on the contrary, if a reference voltage v_c is provided, voltage regulation can be implemented by mean of a PI regulator fed with voltage deviation. In order to obtain integrated virtual inertia and frequency regulation, a PID regulator is necessary to provide reference active power depending on frequency deviation. The PID regulator is considered in the form

$$PID(s) = k_p + \frac{k_i}{s} + s\frac{k_d}{1+s/N} \tag{9}$$

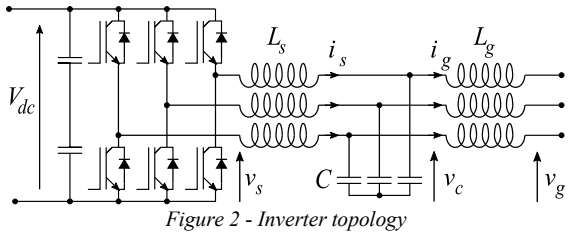

Figure 2 - Inverter topology

where k_p, k_i and k_d are, respectively, the proportional, integral and derivative gains and N is the additional pole frequency, to be chosen accordingly to the desired bandwidth. The global microgrid control scheme comprising converter and synchronous generator regulators is reported in Fig.3. To realize virtual inertia, the synchronous machine rotor swing equation will be considered in order to design the derivative action coefficient k_d. The swing equation can be written in its linearized form [38] as

$$P_m - P_e = J\omega_s \frac{d\omega}{dt} + B\omega \tag{10}$$

where P_m is mechanical power, P_e is electrical power, J is rotor moment of inertia, ω is rotor angular speed, ω_s is synchronism angular speed and B is the friction factor. The derivative action can hence be approximated by the product of rotor moment of inertia J and synchronism angular speed ω_s, namely $k_d = J\omega_s$. Consequently, the derivative action coefficient k_p should be chosen according to

$$k_d = J_{eq}\omega_s \tag{11}$$

so that an equivalent rotor inertia J_{eq} is emulated during the frequency transients. Proportional and integral coefficients k_p and k_i will be chosen in order to obtain efficient primary and secondary regulation. Proportional gain k_p should be chosen in order to provide a reasonable droop and can be obtained from

$$k_p = \frac{P_{inv}}{\sigma\omega_s} \tag{12}$$

where P_{inv} is the inverter rated power and σ is the droop coefficient. This approach allows to run the regulator as PD if necessary: in this case, which is usually limited to grid-connected operation, the converter control is reduced to traditional droop control with inertia emulation by setting the integral term k_i to zero. On the contrary, during islanded operation, the integral gain can be obtained by mean of the integral action time constant T_I by means of

$$k_i = \frac{k_p}{T_I} \tag{13}$$

Note that the integral term is not strictly necessary, in that the speed governor of the synchronous generator would eventually restore frequency nominal value even if the integral gain is set to zero. Furthermore, if the micro-grid is operated in grid-connected mode, the integral term should be set to zero to allow for load sharing based on droop coefficients. Nevertheless, in this paper an integral term is adopted since, in islanded micro-grids, it introduces a further degree of freedom in frequency control which is not affected by mechanical constraints; in fact, the integral term allows to control how the frequency nominal value is restored and hence obtain better dynamic performances, especially when the considered micro-grid is supplied by weaker generators. In order to perform secondary regulation, which is necessary when frequency regulation is based on storage devices or when higher level optimization is performed, a PI regulator (Fig.3) is introduced to perform steady-state active power control. To allow for efficient frequency regulation, this second regulator should have significantly lower bandwidth than frequency regulation, which drastically increase transient duration but keep frequency deviation into a smaller range. Faster secondary regulation can be performed to reduce storage device sizing, but this would clearly interfere with primary frequency regulation. Note that, in case of grid–connected operation, the secondary regulator should also be deactivated in order to allow the global control to be operated as a pure PD (i.e. droop control with virtual inertia).

B. Voltage and frequency regulation in micro-grids with little or no synchronous generation

Since no synchronous generators are present in this case, there's no need to realize traditional voltage and frequency regulation. As long as microgrids with few power sources are considered, one could eventually contemplate fixed frequency operation in order to avoid frequency-related issues and maximize grid stability. Clearly, due to fixed frequency operation, this solution does not directly guarantee correct power sharing among converters, but this issue can be addressed by mean of a hierarchical control structure [37]. Hence, to maximize frequency and voltage stability, the proposed control strategy consists of a master converter (inverter 2) which imposes constant frequency and voltage and a slave converter (inverter 1) which injects a predefined active and reactive power into the grid (Fig.1,b). Inverter 1 control is very similar to case A in that it is required to exchange a predefined active and reactive power. In this second case, reference active power is constant since frequency regulation is not needed, while reference reactive power is obtained from a voltage regulator as in the previous case. On the contrary, Inverter 2 should behave as a high-performance voltage source. For this reason, a pseudo sliding-mode approach has been chosen for its high dynamic and stability performances. Detailed discussion on this control approach can be found in [32], [33], [43], [44]. Furthermore, this approach can be easily extended to modular converters to obtain greater flexibility, fault resilience, harmonic distortion cancellation and power transfer capabilities [45]-[47]. Considering voltage phase and frequency, there are no specific issues as long as the converter

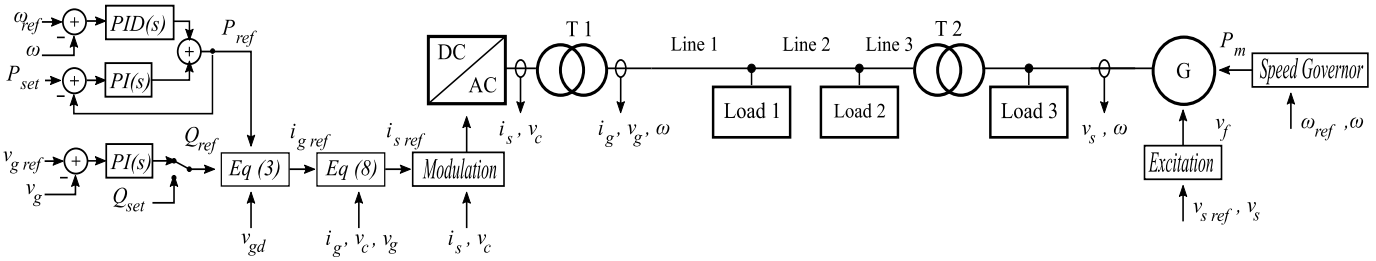

Figure 3 – Converter control for voltage and frequency regulation in micro-grids with prevalent synchronous generation

is operated at fixed frequency. In this case frequency can be chosen arbitrarily, generally equal to its nominal value, and reference phase is obtained from frequency integral over time with arbitrary initial condition. Current references for the modulation algorithm are obtained with an inverse dynamic approach, analogously to the previously illustrated current control. The resulting microgrid control scheme is reported in Fig.4. Now let us focus on inverter 2 voltage control. Defined the voltage tracking error as

$$\varepsilon_v = \boldsymbol{v}_{c\ ref} - \boldsymbol{v}_c \tag{14}$$

it is then possible to write the dynamic voltage error equation

$$\eta_v = \varepsilon_v + T_{v1} \cdot \dot{\varepsilon}_v + \frac{1}{T_{v2}} \int \varepsilon_v \, dt \tag{15}$$

where T_{v1}, and T_{v2} are coefficients to be chosen in order to obtain the desired damping and dynamic response. Considering the capacitors constitutive relations, it is easy to prove that

$$\dot{\varepsilon}_v = \dot{\boldsymbol{v}}_{c\ ref} + j\omega \boldsymbol{v}_c + \frac{1}{C}\left(\boldsymbol{i}_g - \boldsymbol{i}_s\right) \tag{16}$$

In (16) only the reference voltage derivative is present and it can be easily obtained since the reference is calculated in the control. Substituting (16) and (14) in (15) and imposing $\eta_v=0$ and $\boldsymbol{i}_s = \boldsymbol{i}_{s\ ref}$, it is possible to obtain the current reference $\boldsymbol{i}_{s\ ref}$ as

$$\begin{aligned} \boldsymbol{i}_{s\ ref} = &\left[C\dot{\boldsymbol{v}}_{c\,ref} + j\omega C \boldsymbol{v}_c + \boldsymbol{i}_g \right] + \\ &+ g_{v1} C\left(\boldsymbol{v}_{c\ ref} - \boldsymbol{v}_c\right) + g_{v2} C \int \left(\boldsymbol{v}_{c\ ref} - \boldsymbol{v}_c\right) dt \end{aligned} \tag{17}$$

where gains are defined as $g_{v1}=1/T_{v1}$, $g_{v2}=1/(T_{v1}T_{v2})$. It is possible to determine gain values considering (15) in frequency domain with $\eta_v=0$; it is not difficult to prove that optimal damping is obtained when $g_{v1}=2/T$, $g_{v2}=1/T^2$, where T is the desired system time constant, which can be chosen as reported in the previous paragraph. Overall, the control is equivalent to a PI regulator with a feed-forward/compensation term: in (17) the first term can be considered a feed-forward/compensation term, while the second and third terms are, respectively, proportional and integral terms. The impact of the proposed method on the stability of the system will be discussed in the Section IV, A as well.

IV. Stability Analysis

A. Voltage control stability

Let us consider voltage control firstly for simplicity. The controlled system can be written in normal form isolating real and imaginary components of space vectors as

$$\begin{cases} \dot{x}_v = \mathbf{A}_v x_v + \mathbf{B}_v u_v + \mathbf{M}_v d_v \\ y_v = x_v \end{cases} \tag{18}$$

where $x_v=[v_{cd}\ v_{cq}]^T$, $u_v=[i_{sd}\ i_{sq}]^T$, $d_v=[i_{gd}\ i_{gq}]^T$ and

$$\mathbf{A}_v = \begin{bmatrix} 0 & \omega \\ -\omega & 0 \end{bmatrix},\ \mathbf{B}_v = \frac{1}{C}\mathbf{I}_2,\ \mathbf{M}_v = -\mathbf{B}_v \tag{19}$$

with $\mathbf{I}_m$ representing a m×m identity matrix. Define now an auxiliary state w_v such that

$$\dot{w}_v = y_{v\ ref} - y_v \tag{20}$$

Assuming $\boldsymbol{i}_s = \boldsymbol{i}_{s\ ref}$, it is possible to write (17) in matrix form as

$$u_v = i_{s\ ref} = \frac{1}{T_{v1}} \mathbf{B}^{-1} \cdot \left[y_{v\ ref} - x_v - T_{v1}\left(\mathbf{A}_v x_v + \mathbf{M}_v d_v\right) + \frac{1}{T_{v2}} w_v \right] \tag{21}$$

Considering now (18), (20), substituting (21) in (18) and assuming, just for stability considerations, $y_{v\ ref}=0$ and $d_v=0$, after few calculation it is possible to write the extended dynamic system as

$$\begin{cases} \dot{x}_v = -g_{v1}\mathbf{I}_2\, x_v + g_{v2}\mathbf{I}_2\, w_v \\ \dot{w}_v = -x_v \\ y_v = x_v \end{cases} \tag{22}$$

The extended dynamic matrix is then obtained as

$$\mathbf{A}_v{}' = \begin{bmatrix} -g_{v1}\mathbf{I}_2 & g_{v2}\mathbf{I}_2 \\ -\mathbf{I}_2 & \mathbf{0}_2 \end{bmatrix} \tag{23}$$

with $\mathbf{0}_m$ representing a m×m null matrix. The characteristic polynomial of $\boldsymbol{A}_v'$ results in

$$\det(s\mathbf{I}_4 - \mathbf{A}_v{}') = \left(s^2 + g_{v1}s + g_{v2}\right)^2 \tag{24}$$

Considering (24), it is easy to prove that the roots of the characteristic polynomial have negative real part as long as gains g_{v1}, g_{v2} are positive, which is granted with the adopted tuning method, and hence the controlled system is asymptotically stable. It is also highlighted that the eigenvalues of the dynamic matrix are assigned by choosing gains g_{v1}, g_{v2}, so that the internal dynamics can be arbitrarily assigned. Note that these results are obtained assuming $\boldsymbol{i}_s = \boldsymbol{i}_{s\ ref}$, which implies that their validity is intrinsically limited to the low frequency behaviour of the system (i.e. system behaviour neglecting switching ripple) and subject to the capability of the converter.

B. Current control stability

Let us now consider the current control, following the same path adopted for voltage control stability analysis. The controlled system can be written in normal form as

$$\begin{cases} \dot{x}_i = \mathbf{A}_i x_i + \mathbf{B}_i u_i + \mathbf{M}_i d_i \\ y_i = \mathbf{C} x_i \end{cases} \tag{25}$$

where $x_i=[v_{cd}\ v_{cq}\ i_{gd}\ i_{gq}]^T$, $u_i=[i_{sd}\ i_{sq}]^T$, $d_i=[v_{gd}\ v_{gq}]^T$ and

$$\mathbf{A}_i = \begin{bmatrix} \mathbf{A}_v & -\frac{1}{C}\mathbf{I}_2 \\ \frac{1}{L_g}\mathbf{I}_2 & \mathbf{A}_v \end{bmatrix}, \mathbf{B}_i = \begin{bmatrix} \frac{1}{C}\mathbf{I}_2 \\ \mathbf{0}_2 \end{bmatrix}, \mathbf{C}_i = \begin{bmatrix} \mathbf{0}_2 & \mathbf{I}_2 \end{bmatrix}, \mathbf{M}_i = \begin{bmatrix} \mathbf{0}_2 \\ -\frac{1}{L_g}\mathbf{I}_2 \end{bmatrix} \tag{26}$$

Define now an auxiliary state w_i such that

$$\dot{w}_i = y_{i\ ref} - y_i \tag{27}$$

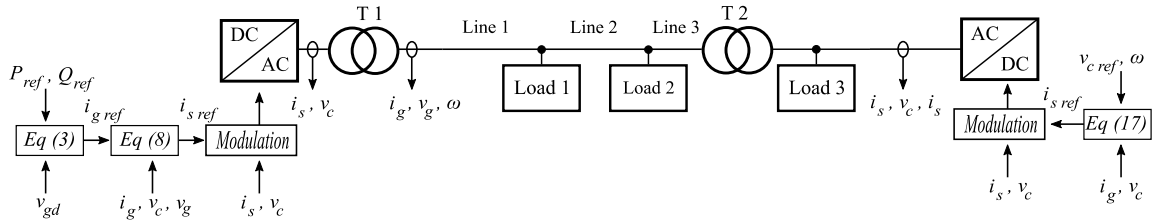

Figure 4 – Converter control for voltage and frequency regulation in micro-grids with little or no synchronous generation

Assuming $\boldsymbol{i}_s=\boldsymbol{i}_{s\,ref}$, $y_{i\,ref}=0$ and $d_i=0$, (8) can be rearranged as

$$u_i = \frac{1}{T_{i2}}\left[\mathbf{C}_i\mathbf{A}_i\mathbf{B}_i\right]^{-1}\cdot\left[-\mathbf{C}_i x_i - T_{i1}\mathbf{C}_i\mathbf{A}_i x_i - T_{i2}\mathbf{C}_i\mathbf{A}_i\mathbf{A}_i + \frac{1}{T_{i3}}w_i\right] \quad (28)$$

Considering now (25), (27) and (28), after some calculation the extended dynamic system can be obtained as

$$\begin{cases}\dot{x}_i = \mathbf{A}_{1i}x_i + \mathbf{A}_{2i}w_i \\ \dot{w}_i = -\mathbf{C}_i x_i \\ y_i = \mathbf{C}_i x_i\end{cases} \quad (29)$$

where

$$\mathbf{A}_{1i} = \left[\mathbf{A}_i - \frac{1}{T_{i2}}\mathbf{B}_i\left[\mathbf{C}_i\mathbf{A}_i\mathbf{B}_i\right]^{-1}\mathbf{C}_i - \frac{T_{i1}}{T_{i2}}\mathbf{B}_i\left[\mathbf{C}_i\mathbf{A}_i\mathbf{B}_i\right]^{-1}\mathbf{C}_i\mathbf{A}_i + -\mathbf{B}_i\left[\mathbf{C}_i\mathbf{A}_i\mathbf{B}_i\right]^{-1}\mathbf{C}_i\mathbf{A}_i\mathbf{A}_i\right]_{4\times4} \quad (30)$$

$$\mathbf{A}_{2i} = \left[\frac{1}{T_{i2}T_{i3}}\mathbf{B}_i\left[\mathbf{C}_i\mathbf{A}_i\mathbf{B}_i\right]^{-1}\right]_{4\times2} \quad (31)$$

The extended dynamic matrix is then structured as

$$\mathbf{A}_i' = \begin{bmatrix}\mathbf{A}_{1i} & \mathbf{A}_{2i} \\ -\mathbf{C}_i & \mathbf{0}_2\end{bmatrix}_{6\times6} \quad (32)$$

and the characteristic polynomial of $\boldsymbol{A}_i'$ results

$$\det(s\mathbf{I}_6 - \mathbf{A}_i') = \left(s^3 + g_{i1}s^2 + g_{i2}s + g_{i3}\right)^2 \quad (33)$$

Considering (33), it is easy to prove that the zeros of the characteristic polynomial have negative real part as long as gains g_{i1}, g_{i3} are positive and $g_{i2}>g_{i3}/g_{i1}$, which is granted with the adopted tuning method, and that the eigenvalues of the dynamic matrix are assigned by choosing gains g_{i1}, g_{i2}, g_{i3}. Final considerations expressed on voltage control are to be considered valid also for current control.

C. Frequency stability in micro-grids with prevalent synchronous generation

For frequency stability considerations, the dynamics of interest can be modelled through transfer functions. The converter model, neglecting secondary regulation, can be reduced to (9) assuming converter dynamics to be much faster than frequency dynamics. The synchronous machine can be modelled rearranging (10) as

$$G_{Synch}(s) = \frac{1}{\omega_S}\cdot\frac{1}{Js+B} \quad (34)$$

The resulting system frequency regulation block diagram is reported in Fig.5. Considering (34), (1), (9), the closed-loop transfer function can be obtained as

$$L(s) = \frac{G_{Synch}(s)}{1+G_{Synch}(s)\left[PID(s)+G_{Gov}(s)\right]} \quad (35)$$

Considering (9), (34), (35) it is clear than the denominator of the closed-loop transfer function is a fifth grade polynomial, so that analytical pole calculation is pretty complex and their dependence on regulators gain is unclear. Anyway, the transfer function poles can be easily calculated numerically to prove frequency stability.

V. Case Studies

A. First case study: voltage and frequency regulation in micro-grids with prevalent synchronous generation

The grid topology considered for the first case study is shown in Fig.1,a. Generators, loads, and transformers ratings are reported in Table 1. Line parameters are reported in Table 1. The synchronous machine, speed governor and static exciter parameters are reported in Table 2, while the converter circuital parameters and assigned time constants, as long as its active power controller parameters, are reported in Table 3. The proposed control performances will be tested considering a step increase in load 1 power absorption from 500 kW to 1 MW at constant power factor. Simulations are performed in Matlab/Simulink.

B. Second case study: voltage and frequency regulation in micro-grids with little or no synchronous generation

The grid topology considered for this second case study is reported in Fig.1,b and is totally equivalent to study case A except from active users. Generators, loads, and transformer ratings are reported in Table 1. Line parameters are reported in Table 4. The converters circuital parameters and assigned time constants are reported Table 5. Grid operation will be tested considering a step increase in load 1 power absorption from 500 kW to 1 MW in order to allow significant comparison between the two cases. Simulations are performed in Matlab/Simulink.

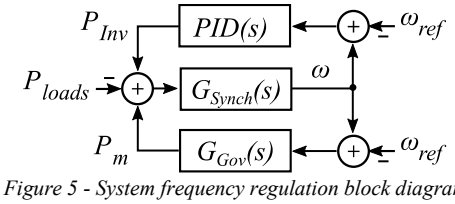

Figure 5 - System frequency regulation block diagram

TABLE 1 - GENERATORS AND LOADS

Case study A	*Case study B*	*Voltage [V]*	*Rated Power*
Inverter	Inverter 1	400 V	1250 kVA
Synch. generator	Inverter 2	400 V	2000 kVA
Load 1		20 kV	1 MW, cosφ=0.95
Load 2		20 kV	1 MW, cosφ=0.95
Load 3		400 V	100 kW, cosφ=0.95
Transformer 1		400/20000	2000 kVA
Transformer 2		400/20000	2000 kVA

TABLE 2 – LINE PARAMETERS

Line	*Type*	*Voltage [kV]*	*Resistance [Ω/km]*	*Reactance [Ω/km]*	*Length [km]*
# 1	*Overhead*	*20*	*1.5*	*0.5*	*2.0*
# 2	*Overhead*	*20*	*1.5*	*0.5*	*2.0*
# 3	*Overhead*	*20*	*1.5*	*0.5*	*1.5*

TABLE 3 – SYNCHRONOUS GENERATOR PARAMETERS

Synchronous Generator		*Speed Governor*		*Exciter*	
Parameter	*Value*	*Par.*	*Value*	*Par.*	*Value*
Nominal Frequency [Hz]	*50*	k_{g1}	*200*	k_e	*2.5*
		k_{g2}	*10*	T_{e1} *[s]*	*0.4*
J [kg·m²]	*49.81*	T_{g1}*[s]*	*0.3*	T_{e2}*[s]*	*0.03*
B [N·m·s]	*0.08*	σ_{synch}	*0.05*		

TABLE 4 – INVERTER PARAMETERS

Converter		*Active Power Controller*		
Parameter	*Value*	*Parameter*	*Value*	
			PD (Fig.6)	*PID (Fig.8)*
f_s *[kHz]*	*10*	σ	*0.05*	*0.05 (red)*
L_s *[mH]*	*0.1*			*0.01 (green, blue)*
L_g *[μH]*	*32.6*	J_{eq} *[kg·m²]*	*0 (red)*	*50 (red)*
C [mF]	*3.1*		*50 (green)*	*250 (green)*
T [s]	*0.002*		*250 (blue)*	*500 (blue)*
f_n *[Hz]*	*50*	T_1 *[s]*	-	*0.100*

VI. SIMULATION RESULTS

A. *First case study: voltage and frequency regulation in micro-grids with prevalent synchronous generation*

At time t=0 the grid is in steady state; at time t=1 s, load 1 increases its power absorption of 500 kW. Fig.6 reports the consequent frequency transient under different converter operation. As a reference, the frequency transient obtained with no converter contribution to frequency regulation is reported in black. Even though nominal frequency is correctly restored, the initial frequency oscillation amplitude is excessively large due to the reduced system inertia. Since in islanded operation relatively large transients are unavoidable, this may represent a significant issue. Traditional solutions to reduce this issue are converter droop control, which is also prescribed by the actual technical normative, and virtual inertia: the former allows to introduce a significant damping, but it is not very effective in reducing the initial frequency drop (Fig.6, red). On the contrary virtual inertia allows to reduce initial frequency drop (Fig.6, green and blue), but increases frequency transient durations since only the synchronous generator is acting to restore frequency nominal value. Clearly, if only equivalent rotor inertia is increased, the converter power contribution is similar to the one obtained with a similarly powered synchronous machine equipped with a heavier rotor: frequency oscillations are smaller, less damped and longer in period. For clarity, the power supplied by the converter and the synchronous generator during the aforementioned transients is reported in Fig.7. Even though this approach allows to obtain acceptable results, it is possible to further exploit converter capabilities in order to not only reduce frequency transient amplitude, but also to control how the nominal frequency is restored by adding an integral term, according to (13), and a secondary regulation loop (Fig.3). Fig.8 reports the consequent frequency transient under different converter operation. For the sake of clarity, the frequency transient obtained with no converter contribution to frequency regulation is reported in black as reference. Firstly, the transient obtained with parameters equal to the previous case with an added integral term is reported in Fig.8, red. In this situation, the frequency transient amplitude is slightly reduced, but its duration is increased due to secondary regulation action, which restores converter power reference in about a minute. Anyway, since the secondary regulation allows to control steady state active power, it is possible to emulate a larger machine (i.e. larger inertia and smaller droop coefficient) in order to reduce frequency perturbations. The consequent results are reported in Fig.8, green and blue. One can notice that maximum frequency deviation is considerably reduced (lower than 100 mHz) and that few seconds after the beginning of the transient frequency deviation is reduced to few tens of mHz. If the proposed approach is applied, frequency transient amplitude and duration are a compromise solution due to inverter necessity to return to reference active power in a

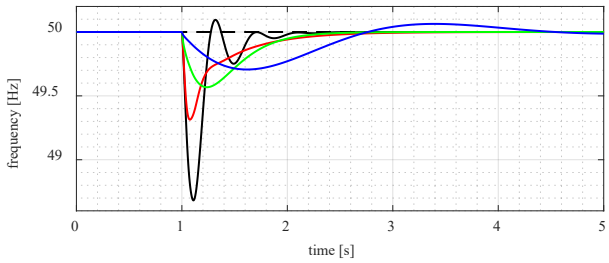

Figure 6 - Frequency transient due to load step: constant inverter power (black), droop control (red, σ=0.05), droop control with virtual inertia (green and blue, σ=0.05, Jeq=50 kg·m2 and Jeq=250 kg·m2, respectively)

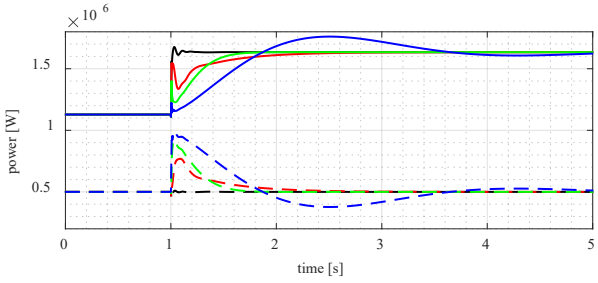

Figure 7- Power transient: synchronous generator (continuous) and inverter (dashed). Constant inverter power (black), droop control (red, σ=0.05), droop control with virtual inertia (green and blue, σ=0.05, J_{eq}=50 kg·m² and J_{eq}=250 kg·m², respectively)

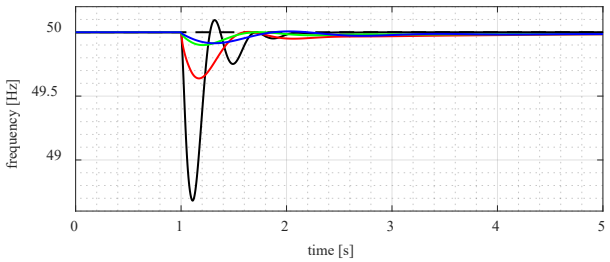

Figure 8- Frequency transient due to load step: constant inverter power (black), proposed PID control with secondary regulation: red (σ=0.05, Jeq=50 kg·m2, Ti=0.1 s), green (σ=0.01, Jeq=250 kg·m2, Ti=0.1 s) and blue (σ=0.01, Jeq=500 kg·m2, Ti=0.1 s).

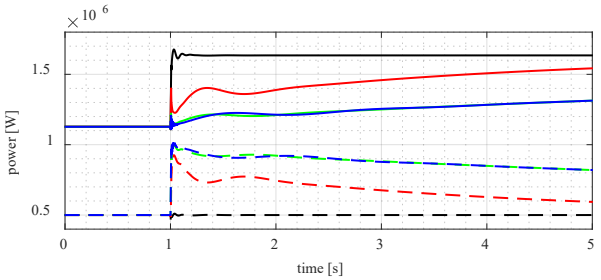

Figure 9- Power transient: synchronous generator (continuous) and inverter (dashed). Constant inverter power (black), proposed PID control with secondary regulation: red (σ=0.05, J_{eq}=50 kg·m^2, T_i=0.1s), green (σ=0.01, J_{eq}=250kgm^2, T_i=0.1s) and blue (σ=0.01, J_{eq}=500kgm^2, T_i=0.1s).

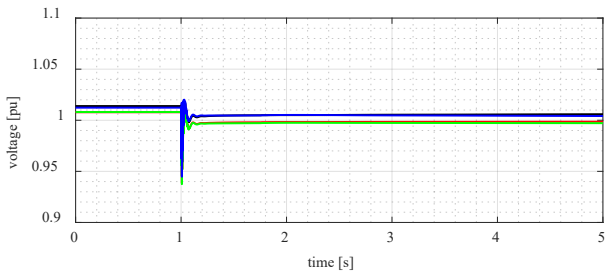

Figure 10 - Voltage transient due to load step: synchronous generator node (black), load 1 node (green), load 2 node (red), converter node (blue)

limited time. Longer recovery time allows smaller frequency deviation but may require excessively large storage devices, while shorter recovery time requires less energy for frequency regulation, but may reduce control effectiveness. For clarity, the power supplied by the converter and the synchronous generator during the aforementioned transients is reported in Fig.9. Comparing the presented results, one can notice that the proposed control allows to significantly increase frequency stability as long as energy storage is available. If not, it is necessary to drastically reduce secondary regulation time constant, which leads to results similar to those obtained through the traditional PD control reported in Fig.8. In both cases, the proposed control allows to completely control frequency transients, both in terms of frequency deviation and transient duration. For the sake of completeness, voltage behaviour corresponding to the transient reported in Fig.8, blue is reported in Fig.10. One can clearly notice that voltage transients are characterized by reduced amplitudes and duration, hence resulting completely acceptable under both technical and normative perspectives. In particular, generator nodes voltages, whose references are set few percent higher than their nominal value, are almost superimposed; load voltages, almost superimposed as well, remain close to their nominal value.

B. Second case study: voltage and frequency regulation in micro-grids with little or no synchronous generation

At time t=0 the grid is in steady state; at time t=1 s, load 1 increases its power absorption of 500 kW. Fig.11 and Fig.12 report, respectively, voltage and power transients due to load 2 increased power absorption. One can notice that, due to the high-performance converter control, voltage transients are even smaller than in the previous case and consequently result completely acceptable. Generator nodes voltages, set few percent higher than their nominal value, are almost superimposed; load voltages, almost superimposed as well, remain close to their nominal value. Furthermore, as expected, converter 1 exchanged power is constant except from a negligible transient, while converter 2 power varies to fulfill the load request. Note that the proposed master-slave approach exhibits high stability and dynamic properties which allow to obtain far better performances with respect to droop-based control approaches, in that voltage are kept almost constant with no need for secondary regulation and negligible transients. Furthermore, frequency is kept constant, which would be impossible for both droop-based controls and virtual synchronous generators. It is also possible to observe that the proposed control does not perform load sharing between the different converters, but this issue may be addressed with a secondary regulation structure or a hierarchical control structure if necessary. Note also that the proposed control may encounter some issue if applied to a grid with many small generators and few large loads, in that it may not be possible to have a master converter in the traditional sense. This issue may be addressed with more sophisticated control approaches if necessary, but in medium voltage grids the generation is usually constituted by few relatively larger generators.

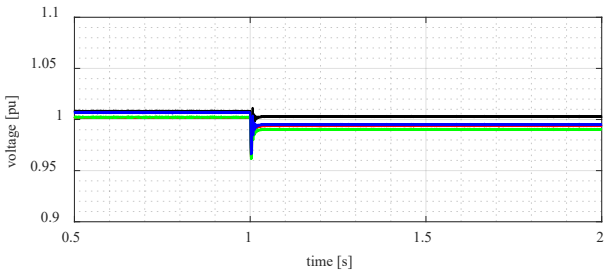

Figure 11- Voltage transient due to load step: converter 2 node (black), load 1 node (green), load 2 node (red), converter 1 node (blue)

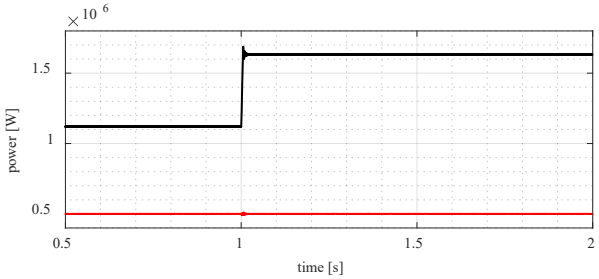

Figure 12- Power transient: master (black) and slave (red) converter

C. *Voltage and current tracking*

Correct voltage tracking achievement has been verified considering the same condition of section VI, paragraph B. The resulting voltage behavior is reported in Fig.13. Current tracking has been verified with a 500 kW reference step for uniformity, and the resulting behavior is reported in Fig.14. One can notice that, for both voltage and current, efficient tracking is achieved. Voltage, in particular, is extremely stable, as one can expect since no approximations are present in control equations. Furthermore, the dynamic cancellation is complete since, with the considered parameters, the maximum derivative of the grid current $\boldsymbol{i}_g$ is lower than the maximum current derivative generated by the converter, and hence controllability condition in maintained during the whole transient. Current tracking is almost as effective as voltage tracking even though minor approximations are present in current control equation, since grid voltage derivative has been neglected. As expected, current does not present significant oscillations.

VII. Conclusion

This paper proposes two control strategies to obtain voltage and frequency regulation in two different islanded-operated grid topologies: the first one considers a grid where synchronous generation is prevalent, while the second considers a grid where synchronous generation is absent. In the first case study, where frequency stability is the main issue, the proposed control effectively reduces frequency deviation and frequency oscillations. Even though the proposed control strategy has been developed for a grid with only two generators, it can easily be extended to grid with many static converters, since the gains of the PID regulator used for frequency regulation depends on the converter rated power and equivalent inertia, that can be considered project parameters. In the second case, where voltage stability is the main issue because of fixed frequency operation, voltage transients are successfully restrained. Better results in load sharing between converters can be obtained with different approaches, but, as long as the master converter is capable of fulfilling load changes, master-slave approach assures maximum service quality. Furthermore, this approach can be easily extended to grids where synchronous generation is present but static generation is prevalent. With respect to traditional control approaches, such as virtual synchronous generators and droop controls, the proposed approach allows to obtain higher voltage and frequency stability. Furthermore, since power flows can be prescheduled, the proposed control is suitable for integration in hierarchical control structures in order to obtain optimized grid operation. In conclusion and with reference to simulation results, the proposed control strategies allow islanded operation in both examined situations in full compliance normative prescriptions and high voltage and frequency stability. Future work will consider higher control layers for grid optimization and islanding/resynchronization management. A hierarchical control structure capable of realizing optimized grid operation in both islanded and grid-connected mode is currently under development and will be object of future publication.

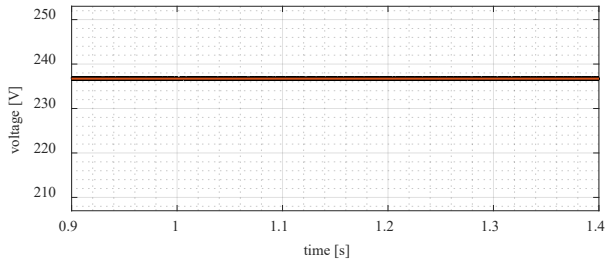

Figure 13 - Master converter filter capacitors voltage (v_c) tracking: reference (red) and measured value (black)

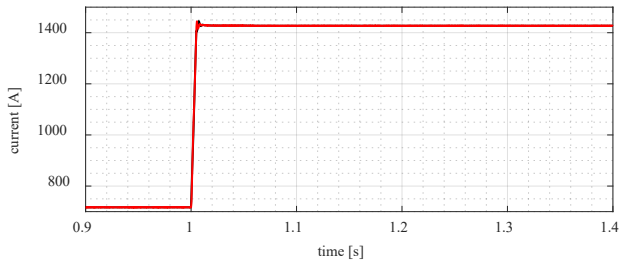

Figure 14 - Slave converter transformer current (i_g) tracking: reference (red) and measured value (black)

References

[1] S. Grillo, V. Musolino, L. Piegari, E. Tironi, C. Tornelli, "DC Islands in AC Smart Grids," *in IEEE Transactions on Power Electronics*, vol. 29, no. 1, pp. 89-98, Jan. 2014

[2] L. Piegari, P. Tricoli, "A control algorithm of power converters in smart-grids for providing uninterruptible ancillary services," *Proceedings of 14th International Conference on Harmonics and Quality of Power - ICHQP 2010*, Bergamo, 2010, pp. 1-7.

[3] M. Corti, A. Massi Pavan, G. Sulligoi, G. Superti Furga, E.Tironi, "Intentional Islanding in Medium Voltage Distribution Grid", *2016 IEEE 16th International Conference on Environment and Electrical Engineering (EEEIC)*, Florence, 2016, pp. 1-6.

[4] CEI 0-16, Reference technical rules for the connection of active and passive consumers to the HV and MV electrical networks of distribution Company, 2014 (in Italian)

[5] CEI 0-16; V2, Reference technical rules for the connection of active and passive consumers to the HV and MV electrical networks of distribution Company, 2016 (in Italian)

[6] CEI 0-21, Reference technical rules for the connection of active and passive users to the LV electrical utilities, 2016 (in Italian)

[7] Q. C. Zhong and G. Weiss, "Synchronverters: Inverters That Mimic Synchronous Generators," in *IEEE Transactions on Industrial Electronics*, vol. 58, no. 4, pp. 1259-1267, April 2011.

[8] Q. C. Zhong, G. C. Konstantopoulos, B. Ren and M. Krstic, "Improved Synchronverters with Bounded Frequency and Voltage for Smart Grid Integration," in *IEEE Transactions on Smart Grid*, vol. 9, no. 2, pp. 786-796, March 2018.

[9] Q. C. Zhong, P. L. Nguyen, Z. Ma and W. Sheng, "Self-Synchronized Synchronverters: Inverters Without a Dedicated Synchronization Unit," in *IEEE Transactions on Power Electronics*, vol. 29, no. 2, pp. 617-630, Feb. 2014.

[10] V. Natarajan and G. Weiss, "Synchronverters With Better Stability Due to Virtual Inductors, Virtual Capacitors, and Anti-Windup," in *IEEE Transactions on Industrial Electronics*, vol. 64, no. 7, pp. 5994-6004, July 2017.

[11] H. Bevrani, T. Ise, and Y. Miura, "Virtual synchronous generators: A survey and new perspectives," *International Journal of Electrical Power & Energy Systems*, vol. 54, pp. 244-254, 1// 2014.

[12] S. Barcellona, Y. Huo, R. Niu, L. Piegari, E. Ragaini, "Control strategy of virtual synchronous generator based on virtual impedance and band-pass damping", *2016 International Symposium on Power Electronics, Electrical Drives, Automation and Motion (SPEEDAM)*, Anacapri, 2016, pp. 1354-1362.

[13] J. Liu, Y. Miura, H. Bevrani and T. Ise, "Enhanced Virtual Synchronous Generator Control for Parallel Inverters in Microgrids," in *IEEE Transactions on Smart Grid*, vol. 8, no. 5, pp. 2268-2277, Sept. 2017.

[14] T. Shintai, Y. Miura and T. Ise, "Oscillation Damping of a Distributed Generator Using a Virtual Synchronous Generator," in *IEEE Transactions on Power Delivery*, vol. 29, no. 2, pp. 668-676, April 2014.

[15] M. Guan, W. Pan, J. Zhang, Q. Hao, J. Cheng and X. Zheng, "Synchronous Generator Emulation Control Strategy for Voltage Source Converter (VSC) Stations," in *IEEE Transactions on Power Systems*, vol. 30, no. 6, pp. 3093-3101, Nov. 2015.

[16] L. M. Castro and E. Acha, "On the Provision of Frequency Regulation in Low Inertia AC Grids Using HVDC Systems," in *IEEE Transactions on Smart Grid*, vol. 7, no. 6, pp. 2680-2690, Nov. 2016.

[17] Y. Cao *et al*., "A Virtual Synchronous Generator Control Strategy for VSC-MTDC Systems," in *IEEE Transactions on Energy Conversion*, vol. 33, no. 2, pp. 750-761, June 2018.

[18] J. Fang, Y. Tang, H. Li and X. Li, "A Battery/Ultracapacitor Hybrid Energy Storage System for Implementing the Power Management of Virtual Synchronous Generators," in *IEEE Transactions on Power Electronics*, vol. 33, no. 4, pp. 2820-2824, April 2018.

[19] Y. Ma, W. Cao, L. Yang, F. F. Wang and L. M. Tolbert, "Virtual Synchronous Generator Control of Full Converter Wind Turbines With Short-Term Energy Storage," in *IEEE Transactions on Industrial Electronics*, vol. 64, no. 11, pp. 8821-8831, Nov. 2017.

[20] N. Soni, S. Doolla and M. C. Chandorkar, "Improvement of Transient Response in Microgrids Using Virtual Inertia," in *IEEE Transactions on Power Delivery*, vol. 28, no. 3, pp. 1830-1838, July 2013.

[21] N. Soni, S. Doolla and M. C. Chandorkar, "Inertia Design Methods for Islanded Microgrids Having Static and Rotating Energy Sources," in *IEEE Transactions on Industry Applications*, vol. 52, no. 6, pp. 5165-5174, Nov.-Dec. 2016.

[22] M. Benidris, J. Mitra, "Enhancing stability performance of renewable energy generators by utilizing virtual inertia," *2012 IEEE Power and Energy Society General Meeting*, San Diego, CA, 2012, pp. 1-6.

[23] E. Rakhshani and P. Rodriguez, "Inertia Emulation in AC/DC Interconnected Power Systems Using Derivative Technique Considering Frequency Measurement Effects," in *IEEE Transactions on Power Systems*, vol. 32, no. 5, pp. 3338-3351, Sept. 2017.

[24] M.F.M. Arani, E.F. El-Saadany, "Implementing Virtual Inertia in DFIG-Based Wind Power Generation, in *IEEE Transactions on Power Systems,,* vol. 28, no. 2, pp. 1373-1384, May 2013

[25] J. Zhao, X. Lyu, Y. Fu, X. Hu and F. Li, "Coordinated Microgrid Frequency Regulation Based on DFIG Variable Coefficient Using Virtual Inertia and Primary Frequency Control," in *IEEE Transactions on Energy Conversion*, vol. 31, no. 3, pp. 833-845, Sept. 2016.

[26] M. Ashabani, F. D. Freijedo, S. Golestan and J. M. Guerrero, "Inducverters: PLL-Less Converters With Auto-Synchronization and Emulated Inertia Capability," in *IEEE Transactions on Smart Grid*, vol. 7, no. 3, pp. 1660-1674, May 2016.

[27] W. Wu *et al*., "A Virtual Inertia Control Strategy for DC Microgrids Analogized With Virtual Synchronous Machines," in *IEEE Transactions on Industrial Electronics*, vol. 64, no. 7, pp. 6005-6016, July 2017.

[28] J. M. Guerrero, J. C. Vasquez, J. Matas, L. G. de Vicuna, M. Castilla, "Hierarchical Control of Droop-Controlled AC and DC Microgrids - A General Approach Toward Standardization", in *IEEE Transactions on Industrial Electronics*, vol. 58, no. 1, pp. 158-172, Jan. 2011.

[29] W. Wang, Y. Li, Y. Cao, U. Häger and C. Rehtanz, "Adaptive Droop Control of VSC-MTDC System for Frequency Support and Power Sharing," in *IEEE Transactions on Power Systems*, vol. 33, no. 2, pp. 1264-1274, March 2018.

[30] Giovanni M. Foglia, Luisa Frosio, Matteo F. Iacchetti, Roberto Perini, "Control loop design in a grid supporting mode inverter connected to a microgrid", *2015 17th European Conference on Power Electronics and Applications (EPE'15 ECCE-Europe)*, Geneva, 2015, pp. 1-10.

[31] X. Tang, X. Hu, N. Li, W. Deng, G. Zhang, "A Novel Frequency and Voltage Control Method for Islanded Microgrid Based on Multienergy Storage", in *IEEE Transactions on Smart Grid*, vol. 7, no. 1, pp. 410-419, Jan. 2016.

[32] M. Cucuzzella, G.P.Incremona, A. Ferrara, "Design of Robust Higher Order Sliding Mode Control for Microgrids", ," in *IEEE Journal on Emerging and Selected Topics in Circuits and Systems*, vol. 5, no. 3, pp. 393-401, Sept. 2015

[33] M. Cucuzzella, G.P.Incremona, A. Ferrara, "Decentralized Sliding Mode Control of Islanded AC Microgrids With Arbitrary Topology", in *IEEE Transactions on Industrial Electronics*, vol. 64, no, 8, pp. 6706-6713 Aug. 2017.

[34] J. Liu, Y. Miura and T. Ise, "Comparison of Dynamic Characteristics Between Virtual Synchronous Generator and Droop Control in Inverter-Based Distributed Generators," in *IEEE Transactions on Power Electronics*, vol. 31, no. 5, pp. 3600-3611, May 2016.

[35] C. Andalib-Bin-Karim, X. Liang and H. Zhang, "Fuzzy-Secondary-Controller-Based Virtual Synchronous Generator Control Scheme for Interfacing Inverters of Renewable Distributed Generation in Microgrids," in *IEEE Transactions on Industry Applications*, vol. 54, no. 2, pp. 1047-1061, March-April 2018.

[36] A. La Bella, S. Raimondi Cominesi, C. Sandroni, R. Scattolini, "Hierachichal Predictive Control of Microgrids in Islanded Operation", in *IEEE Transactions on Automation Science and Engineering*, vol. 14, no. 2, pp. 536-546, April 2017.

[37] A. La Bella, S. Negri, R. Scattolini and E. Tironi, "A Two-Layer Control Architecture for Islanded AC Microgrids with Storage Devices," *2018 IEEE Conference on Control Technology and Applications (CCTA)*, Copenhagen, Denmark, 2018, pp. 1421-1426.

[38] F. Saccomanno, "Electric Power System: Analysis and Control", Wiley-IEEE Press, 2003

[39] Gabrio Superti Furga, Simone Barcellona, Enrico Tironi, "Space-vector Approach in Three-phase Unbalance and Distortion Analysis", *2016 17th International Conference on Harmonics and Quality of Power (ICHQP)*, Belo Horizonte, 2016, pp. 721-726.

[40] M.S. Carmeli, F. Castelli Dezza, G. Superti Furga "Smart modulation: a new approach to power converter control", EPE, Graz, Austria, 27-29 Aug. 2001

[41] M.S. Carmeli, F. Castelli Dezza, G. Superti Furga "Constant frequency current modulation algorithm based on linkage flux" *Power Electronics Specialist Conference, 2003. PESC '03. 2003 IEEE 34th Annual*, 2003, pp. 195-200 vol.1.

[42] S. Negri, E. Tironi, D. Sala Danna, "Integrated Control Strategy for Islanded Operation in Smart Grids: Virtual Inertia and Ancillary Services", *2017 IEEE International Conference on Environment and Electrical Engineering and 2017 IEEE Industrial and Commercial Power Systems Europe (EEEIC / I&CPS Europe), Milan, 2017, pp. 1-6.*

[43] M.S. Carmeli, F. Castelli Dezza, G. Superti Furga "Sliding Mode Control for an innovative universal power conditioner with UPS function", *Proceedings of the IEEE International Symposium on Industrial Electronics*, 2005. ISIE 2005., Dubrovnik, Croatia, 2005, pp. 651-656 vol. 2.

[44] M.S. Carmeli, F. Castelli Dezza, G. Superti Furga "Innovative Capacitive Decoupling for a Universal Power Conditioner based on Two-Shunt-VSI Topology", ," *2006 12th International Power Electronics and Motion Control Conference*, Portoroz, 2006, pp. 1688-1693.

[45] M. Brenna, G.C. Lazaroiu, G. Superti Furga, E.Tironi, "Bidirectional Front End Converter for DG with Disturbance Insensitivity and Islanding-Detection Capability", ," in *IEEE Transactions on Power Delivery*, vol. 23, no. 2, pp. 907-914, April 2008.

[46] M.S. Carmeli, F.Castelli Dezza, G. Superti Furga, "Generalized Decoupling Method for Current-Controlled Multiswitching Sysytems", *IEEE Transactions on Industrial Electronics*, vol. 56, no. 2, pp. 348-359, Feb. 2009.

[47] S. Negri, S. Barcellona and G. Superti-Furga, "Detailed analysis of harmonic distortion in modular three-phase converters: Analytical and numerical evaluation," *2018 18th International Conference on Harmonics and Quality of Power (ICHQP)*, Ljubljana, 2018, pp. 1-7.